Proceedings World Geothermal Congress 2005
Antalya, Turkey, 24-29 April 2005

Use of a Mise-a-la-Masse Survey to Determine New Production Targets in Sibayak Field, Indonesia

Suparno Supriyanto[1], Yunus Daud[2], Sayogi Sudarman[3] and Keisuke Ushijima[1]

[1]Exploration Geophysics Laboratory, Department of Earth Resources Engineering, Graduate School of Engineering,

Kyushu University, 6-10-1 Hakozaki, Higashi-ku, Fukuoka 812-8581, JAPAN

[2]Research Center for Geothermal and Environmental Geosciences, Department of Physics,

Faculty of Mathematics and Natural Sciences, University of Indonesia, Kampus Depok 16424, INDONESIA

[3]Geothermal Division, Pertamina, Jl. Medan Merdeka Selatan No.1 A, Jakarta 10110, INDONESIA

Email: supri@mine.kyushu-u.ac.jp

Keywords: mise-a-la-mase, interpretation, Sibayak field.

ABSTRACT

Sibayak geothermal field is located about 65 km to the southwest of Medan in the North Sumatra Province, Indonesia. Recently, a small-scale geothermal power plant (2 MWe) has been installed in this area. Since electricity demand increases in the North Sumatra Province, Pertamina (Geothermal Division) plans to increase the capacity to 20 MWe in the year 2005. Accordingly, detailed knowledge of the reservoir structure and its extension must be determined. The mise-a-la-masse (MAM) surveys were carried out in this field using the exploration well SBY-1 and the production well SBY-4 to delineate a new production target for further field development. Interpretation of the MAM data was done to correlate the results with formation temperatures and lost circulation zones and finally to image a promising reservoir zone. This interpretation result of MAM data indicates that reservoir zones trends to the north-northeast direction of the study area and shows a good correlation with formation temperature and lost circulation zone. This fact leads us to propose that the best production target for the development of the Sibayak area is characterized by the high temperature, high permeability and high well productivity region marked by the dome- shaped resistivity zone below the conductive cap rocks.

1. INTRODUCTION

There are more than thirty geothermal prospect area widely spreading in Sumatra island, Indonesia. The Sibayak geothermal field (Figure 1) is the first geothermal field developed in Sumatra island under different stages of exploration. The exploration results confirmed that the Sibayak field has potential for further development which the proven capacity is 40 MWe (Sudarman et al, 2000). In 1995, Pertamina installed a small-scale geothermal power plant 2.0 MWe in this area. In addition, through July 1999, 10 exploration and production wells have been drilled. Since electricity demand is increasing in the North Sumatra Province, Pertamina will expand the installed capacity to 20 MWe in the year 2005. For this purpose, a new production target in this area required to be delineated.

The main criteria of the production target are productivity, temperature and permeability. To investigate the best production target, the reservoir structure and possible extension, the Sibayak field has been intensively studied by enhancing interpretation technique of the mise-a-la-masse (MAM) data combined with formation temperature and permeability distribution zone. The results are integrated with the production test data in order to develop the most productive zone of the field. This paper emphasizes the main results of the MAM data interpretation by using residual resistivity distribution map and 3-D inversion analysis objected to the understanding of production zones based on the lateral and vertical resistivity distribution.

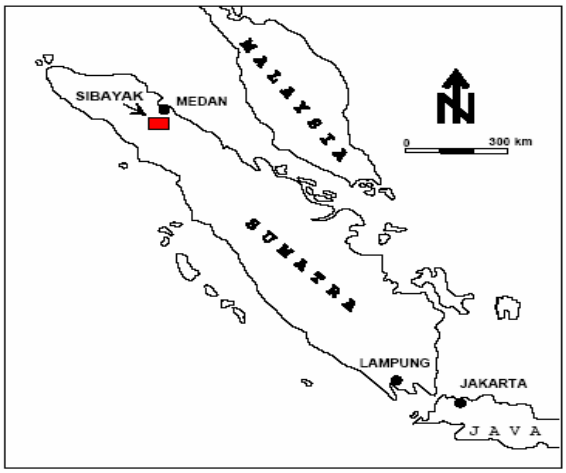

Figure 1: Location map of Sibayak geothermal field.

2. FIELD OVERVIEW

The Sibayak geothermal field including ten-well locations is shown in Figure 5. The field is situated in a high terrain area inside the Singkut caldera. The thermal features consist of solfataras and fumaroles at high elevations around the summit of Mt. Sibayak, and chloride springs with silica sinter at lower elevations in the southern and southeastern of Mt. Pratektekan around the Singkut caldera rim. There has been a complex volcanic history in the area with a number of centers of eruptions developing over a considerable period of time within Quarternary.

In the area of the Singkut caldera, the Quarternary volcanic rock formation is divided into pre and post caldera units. The former includes Singkut dacite-andesite and Singkut laharic breccia, and the latter includes Simpulanangin pyroxene andesite, Pratektekan hornblende andesite Pintau pyroxene andesite and Sibayak hornblende andesite. The volcanic rock formation is composed of andesite, andesite breccia, and tuff breccia. Relatively moderate clay and chloritic hydrothermal alteration are found within this formation.

The geological structure in the Sibayak area is mainly controlled by volcanic and tectonic processes. The caldera structure is elongated to NW-SE (F1 to F4), and it was

developed after the Mt. Singkut volcanic eruption (0.1 Ma). Some fault structures within the caldera are oriented to NW-SE, which is parallel to Great Sumatera Fault, and extend to the center of Mt. Sibayak and Mt. Pintau, where they are intersected by the NE-SW fault structures (F5). The NW-SE fault structures are also intersected by the NE-SW lineament (F6) encountered between Mt Sibayak and Mt Pratektekan.

The locations of fracture zones were identified by the occurrence of lost circulation zones encountered during drilling completion. High lost circulation zones were found in all of existing wells at variable of depths, whereas feed zones were also recognized from the temperature and pressure data. They occur in the north and northeast part of the study area as well as in the southern part outside the singkut caldera rim.

The formation temperatures in the Sibayak geothermal field were measured in the existing wells during well-completion tests. The formation temperature distribution at 300 m depth is shown in Figure 6. The distribution of high temperatures (more than 250^{o}C) occurs to the north beneath Mt. Sibayak and to the northeast beneath Mt. Pratektekan. The highest temperature zone (about 280^{o}C) was observed beneath the eastern flank of Mt. Sibayak near the largest fumaroles in the area.

The permeability distribution map reported by Daud et.al., (2001) in Figure 7 shows that the high permeability area (Kh = 2-4 D.m) is located in the area between Mt. Sibayak and Mt. Pratektekan where many geothermal manifestation found. Meanwhile, the low permeability (Kh = 0.5 D.m) is widely distributed near the Singkut caldera rim.

The production well data of the Sibayak geothermal field as well as the formation temperature data are summarized in the Table 1. The most productive well is SBY-5, whose total production 57 ton/hr steam, which is equivalent to 6 MWe.

Resistivity structures were obtained by two-dimensional (2-D) inversion of MT data (Daud et al., 2000). The resistivity model is characterized by a dome-shaped resistivity (50-200 Ωm) below the strongly altered rock (resistivity of less than 10 Ωm), interpreted as the deep-silicic-prophylitic alteration (reservoir zone).

3. METHOD

Recently, the MAM method has been used in geothermal exploration to map the extent of conductive anomaly zones. The basic idea is to place an electrode inside the geothermal subsurface area and then measure the electric potentials at the surface when current is applied to the electrode. In a geothermal system, hydrothermal fluid flows through high permeability formation such as faults and fractures as well as in horizontal contact between two formations. Moreover, it is observed that hydrothermal fluid has a quite high conductivity, then the faults and fractures itself can be considered as a subsurface conductor (Tagomory et al., 1984). Accordingly, the high permeability zone may have a high conductivity or low resistivity. In the MAM survey, electric current flows easily through a high conductivity medium. As a result, the high permeability zone might be reflected by more conductive anomalous zone recorded by the MAM measurements.

Figure 2 shows the electrode arrangement of the MAM method applied in the geothermal field. The charged current electrode C1 is connected to the anchor well casing to several kilometers depth as a line-current-source in a surveyed area. The distant current C2 is placed at supposedly infinite distance away from the charged current electrode C1. The fixed potential electrode P2 is placed at few kilometers away from the charged well C1 in opposite direction to C2 in order to minimize electromagnetic coupling effects during field survey. Finally, the potential P1 is placed around the well.

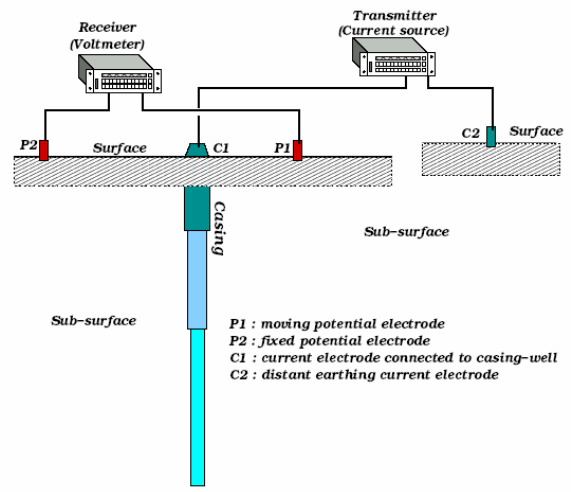

Figure 2: Electrodes arrangement in the MAM survey.

The potential *V* of line-source electrode has been introduced by Kauahikaua et al, (1980). The formula can be derived by process of integration starting from the potential of a point electrode:

$$V = \frac{\rho_a I}{2\pi\lambda}.\ln\left(\frac{\lambda+\sqrt{\lambda^2+r^2}}{r}\right) \qquad (1)$$

Where ρ_a, I, λ, r are the apparent resistivity, the electric current, the length of the line electrode (well casing), and the horizontal distance, respectively. The horizontal distance is measured from the well (C1) at which the potential is measured (P1).

The MAM data can be presented as apparent resistivity distribution, which reflects distribution of gross resistivity in the study area. In order to recognize the response of any subsurface anomalous body, the apparent resistivity value is subtracted by the theoretical resistivity value obtained by linear least square method to get the residual resistivity. According to Daud et al, (2001), the residual resistivity distribution can be laterally interpreted in a correlation with permeability in the study area.

In order to understand the resistivity distribution vertically, Aono at al. (2003) has developed 3-D inversion program, for MAM data using line-source, derived from a non-linear least square method. In the method, unknown parameters can be obtained by a repeated calculation using Marquardt equation:

$$(A^{T}A+\mu C^{T}C)\Delta P \;\square\; A^{T}\Delta g \qquad (2)$$

where **A** is Jacobian matrix, μ is the damping factor, **C** is the smoothing factor, Δ**P** is parameter adjustment vector and Δ**g** is the residual vector. The following procedures have been used for inversion analysis of geophysical data: (1) forward calculation, (2) calculation of Jacobian matrix, (3) least squares method, (4) iterative numerical calculations, and (5) statistical evaluation of solutions. Since, in this procedures, a

large CPU time is necessary for calculating Jacobian matrixes especially in a 3-D inversion, Jacobian matrixes proposed by Loke and Baker (1995) has been used for minimizing a processing time in the program.

4. FIELD MEASUREMENT

The MAM surveys were carried out using the exploratory well SBY-1 and the production well SBY-4. Those wells were selected as a current electrode C1 because the well locations enabled maximum coverage of the field. The total depth of directional wells SBY-1 and SBY-4 are 1501 m (or 1495 m true vertical depth) and 2181 m (or 1879 m true vertical depth), respectively. The electrodes arrangement in field survey is shown in Figure 8. The distant earthed current electrode C2 is fixed at 4.5 km away from the charged well SBY-1 far from the surveyed area to minimize electromagnetic coupling effect. The fixed potential electrode P2 for the current electrode (C1) of charged well SBY-1 was placed to the northeastern part of the surveyed area about 2.5 km away from the well SBY-1. While for the charged well SBY-4, the fixed electrode P2 was located in the northwestern part of survey area 2.5 km away from the well SBY-4.

The potential distribution on the ground surface was measured through potential electrodes P1 and P2. The potential electrode P1 was moved in radial direction from the electrode C1 with 100 m separation. In the Sibayak geothermal field, MAM measurements were conducted along 14 survey lines (163) points around the well SBY-1, whereas around the well SBY-4 the measurements were conducted along 12 survey lines (148 points) as shown in Figure 5. The survey line could not be made in the same length due to field conditions.

The geoelectrical equipment used in this survey was a transmitter with 6 A square wave output, supported by 5 kVA generator power supply, and receiver with reading ability up to 0.01 mV. The potential electrode P1 and P2 were immersed with saturated copper sulfate solution in the porous pots, in order to eliminate the polarization effects during measurement.

5. RESULT

The subsurface resistivity distribution is not homogeneous. It changes laterally and vertically caused by local resistivity structures. Two resistivity inversion techniques were applied in order to get the real resistivity.

Based on 2-D inversion of MT data (Daud et al., 2001), the resistivity structures model is characterized by a dome-shaped resistivity (50-200 Ωm) below the low resistivity zone (less than 10 Ωm). Therefore, the residual resistivity values are calculated by inversion MAM program using the two layer earth model rather than three-layer model in each of the well SBY-1 and SBY-4. Figure 3 shows a map of compilation of residual resistivity distribution from the wells SBY-1 and SBY-4 ranging from -7 to 13 Ωm. By careful inspection to the map, it is obviously recognized that the negative residual resistivity anomaly zone (less than -2 Ωm) is mainly located inside the Singkut caldera, except in the southern part of the area. It could be laterally inferred that the main reservoir may exist at the northwest of the well SBY-1 or at the northeast of the well SBY-4. Moreover, the shape of the negative anomaly coincides with the faulting system. Therefore, the lost circulation zones around the wells SBY-1 and SBY-4 are probably reflected by the NW-SE trending faults. The fault structures also may control the high permeability in the Sibayak area. In addition, another anomaly of low residual resistivity is recognized at the southern part of the Sibayak area, and is interpreted as a permeable zone outside the Singkut caldera margin, which may have a connection to the main reservoir.

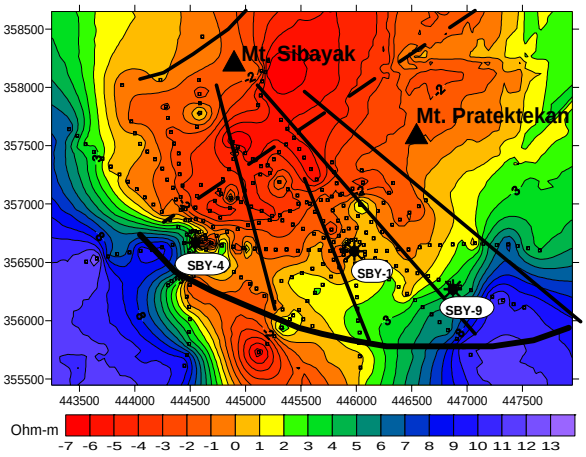

Figure 3: Residual resistivity distribution of the Sibayak geothermal field derived from the MAM measurements.

The 3-D inversion of the MAM data was conducted using a 3-D block model based on the non-linear least squares method. Figure 4 shows some contour resistivity maps variation respect to the depth as a result of the 3-D inversion program. In a shallow depth down to 250 m (Figure 4.A.), the strongly altered rock zones indicated by low resistivity (less than 10 Ωm) are widely distributed in the northern part of the well SBY-4 inside the Singkut caldera. By careful inspection to the map, it is obviously recognized that the low resistivity zone in the northern part of the well SBY-4 follows the NE-SW lineament (F6) encountered between Mt Sibayak and Mt Pratektekan. In the opposite site, a smaller zone of the low resistivity is also found in the southern part of the well SBY-4 separated by Singkut caldera rim. Meanwhile, in the area around the well SBY-1, another small low resistivity zone is found in the eastern part of the well. In the north of the well SBY-1, there is a big area of the low resistivity zone, but because of no MAM stations in that area, it can not be interpreted by the method. In addition, the high resistivity zones (fresh volcanic rock) are mainly located outside the caldera in the southeast and the southwest direction of the Sibayak field.

Figure 4.B shows a block of resistivity at interval depth between 500-750m. It is found that the anomaly low resistivity zone surrounding the well SBY-4 outside the caldera become increase as well as the anomaly in the eastern part of the well SBY-1. This phenomenon can be inferred that the rock alteration zones have gradually removed to the north direction. Moreover, the resistivity contour map in the Figure 3.C and the Figure 3.D has also strengthened the above conclusion. Therefore, it can be interpreted that the thickness of the rock alteration zone distributed in the eastern part of the well SBY-1 and the rock alteration outside the Singkut caldera may be less than 1 km.

By comparing all figures in the Figure 4, it is recognized that the lowest resistivity anomaly zone which can be interpreted as a center of geothermal reservoir is located in the area of faulting systems between Mt.Sibayak and Mt.Pratektekan. This area has a good agreement with the permeability map reported by Daud et al, (2001) where the high permeability zone (Kh = 2-4 D.m) encountered by well SBY-5, SBY-6 and SBY-8, is located in the same area.

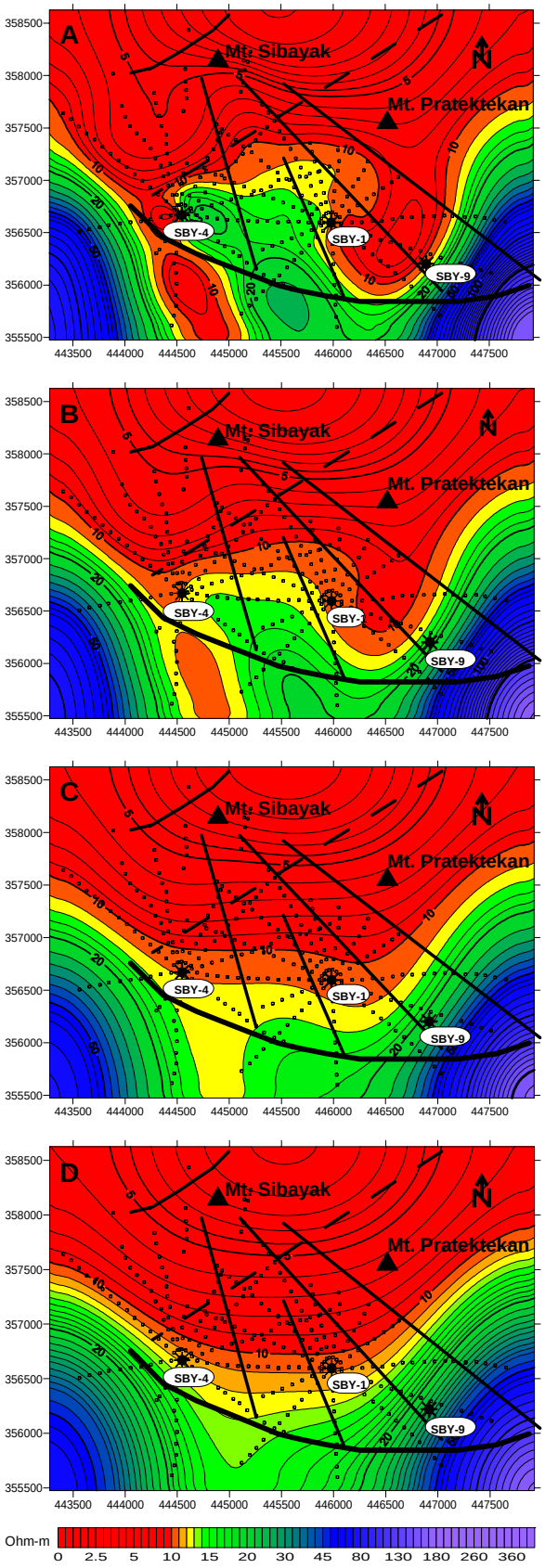

Figure 4: Depth sliced resistivity contour map derived from 3-D inversion of the MAM data. (A) 0-250m (B) 500-750m (C) 1000-1250m (D) 1500-1750m

This result also reflects the faults structure (F1 to F4) which extends to the Mt. Sibayak. Moreover, as shown in Figure 6, this area also has a high formation temperature. On the other hand, the position of bottom well SBY-9 at depth 1527 m is recognized in a higher resistivity than the bottom of the wells SBY-1 and SBY-4. Therefore, its bottom well is located in lower permeability than others. This interpretation has good correlation with the permeability distribution map as shown in the Figure 7. Moreover, the well SBY-9 has produced the smallest amount of steam (15 t/h). Finally, based on all above results, it can be inferred that a future promising geothermal reservoir is located in the subsurface area between Mt. Sibayak and Mt. Pratektekan. Meanwhile, all the maps in Figure 3 also show that the high resistivity zone (fresh volcanic rock) is still distributed in the southeast and the southwest of the Sibayak field where the permeability is low.

6. CONCLUSION

The resistivity structure in the Sibayak geothermal field has been achieved by inversion program derived from least-square method. It is concluded that the trend of low resistivity zone, in variation respect to the depth, extends to the area between Mt. Sibayak and Mt. Pratektekan. The zone has good correlation to the permeability distribution obtained by integrating previous geophysical data. Therefore, this study proposes that the best future production target for the development of the Sibayak area characterized by the high temperature, high permeability and high well productivity region is located beneath of the area between Mt. Sibayak and Mt. Pratektekan.

7. ACKNOWLEDGEMENTS

The authors wish to express their gratitude to the Management of Pertamina (Indonesia) for using the data and their permission to publish this paper. The first author gratefully acknowledges support from a postgraduate scholarship awarded by The Monbukagakusho Scholarship, Japan.

REFERENCES

Sudarman, S., Suroto, Pudyastuti, K. and Aspiyo, S. (1999). Geothermal Development Progress in Indonesia Country Update 1995-2000. *World Geothermal Conference*, Japan, May and June, 2000. Pages 455-460.

Tagomori, K., Ushijima, K. Kinoshita, Y., (1984). Direct Detection of Geothermal Reservoir at Hatchobaru Geothermal Field by The Mise-a-La-Masse Measurement. *Geothermal Resources Council, Transactions*, vol. 8. Pages 65-68.

Kauahikaua, J., Mattice, M., and Jackson, D.,(1980). Mise-a-la-masse mapping of the HGP-A geothermal reservoir, Hawaii. *Geothermal Resources Council, Transactions*, vol 4. Pages 513-516.

Daud, Y., Sudarman, S., Ushijima, K., (2001). Imaging Reservoir Permeability of The Sibayak Geothermal Field, Indonesia Using Geophysical Measurements. *Proceedings 21st Workshop on Geothermal Reservoir Engineering*, Stanford, California. Pages 127-133.

Aono, T., Mizunaga, H., Ushijima, K., (2003). Imaging Fracture during Injection and Production Operations of Reservoirs by a 4-D Geoelectrical Method. Proceedings of the 6th SEGJ International Symposium. Tokyo. Pages 281-287

Daud, Y., Mustopa, E.J., Sudarman, S., Ushijima, K. (2001). 2d Inversion of Magneto-Telluric Data in Sibayak Geothermal Field, Indonesia. *Proceedings of the 105th SEGJ Conference.* Pages 230-233.

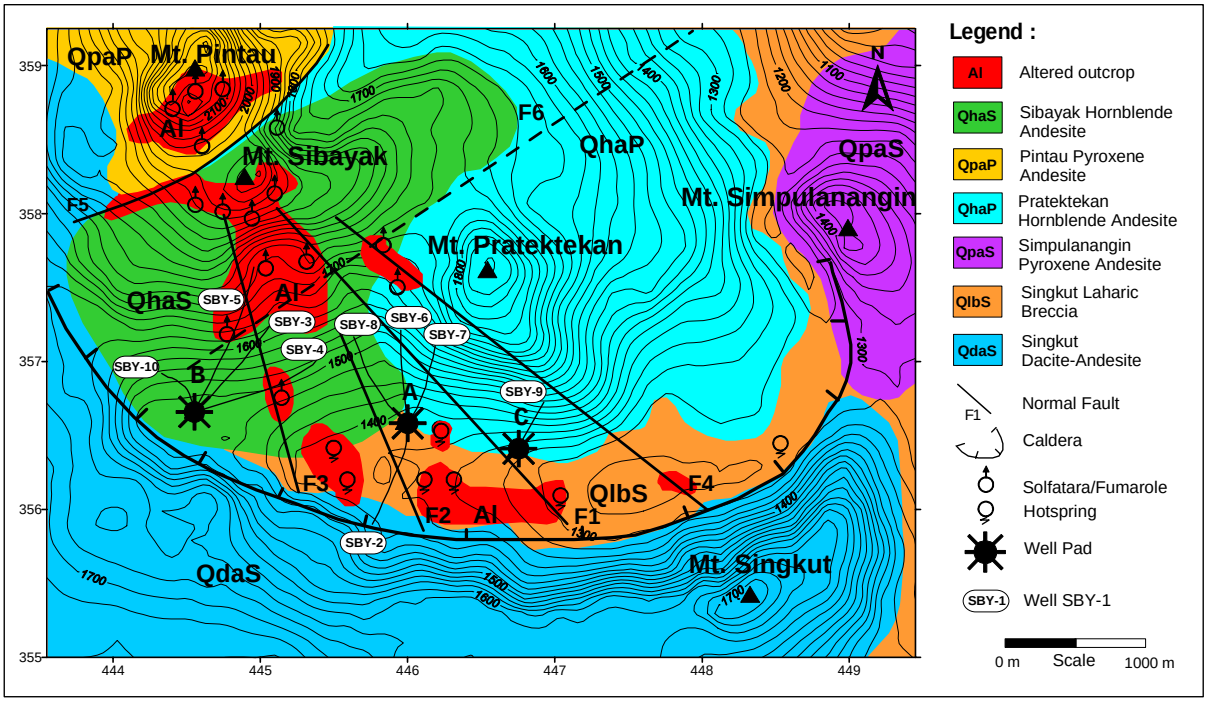

Figure 5: Geological map of Sibayak geothermal field. (Daud et al., 2001)

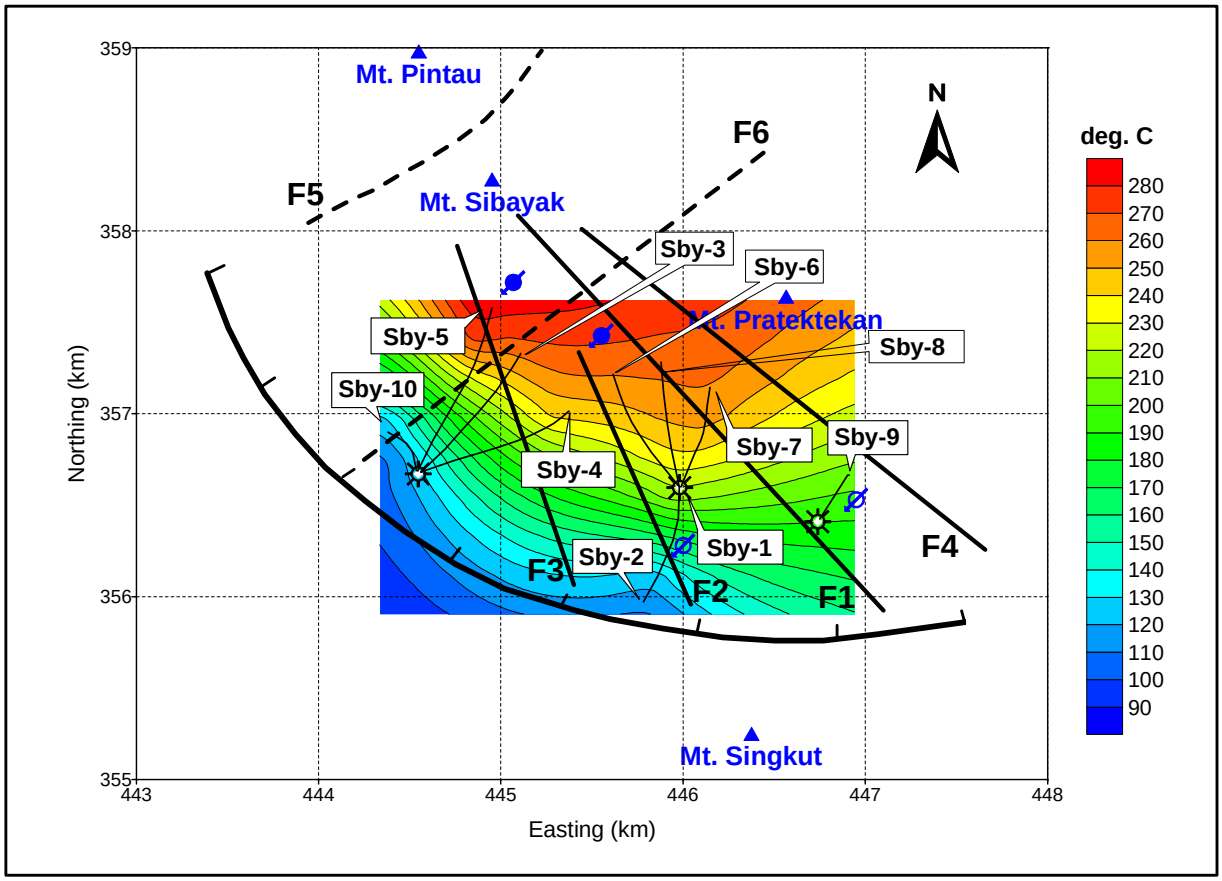

Figure 6: Distribution of the formation temperatures at the elevation of -300 m

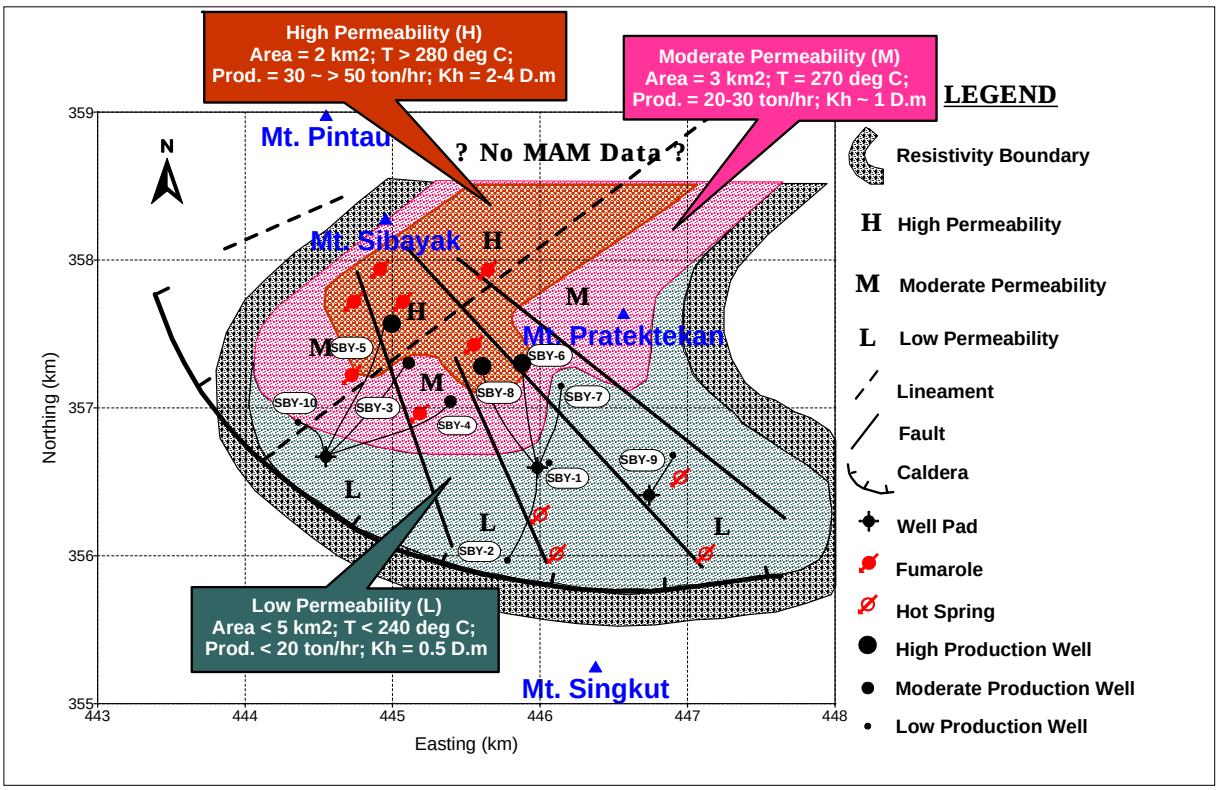

Figure 7: Permeability map of the Sibayak geothermal field.

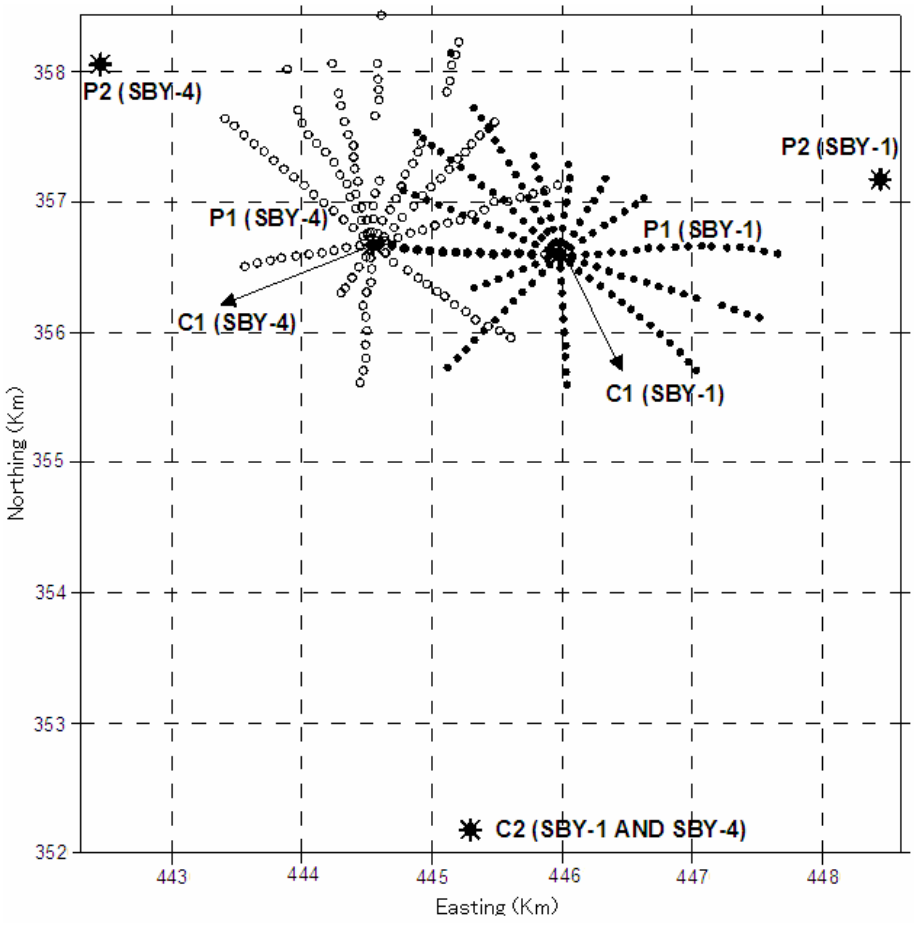

Figure 8: Electrodes arrangement of MAM measurement in the Sibayak field.

Table 1. Production output of the wells in the Sibayak geothermal field.

No	Data	Dimension	SBY-1	SBY-2	SBY-3	SBY-4	SBY-5
1	Type		Exploration	Exploration	Exploration	Development	Development
2	Elevation	m (above sea level).	1384	1384	1468	1468	1384
3	Total depth	m (vertical depth)	1498	2116	1880	1880	1994
4	Temp. at total depth	^{o}C	243	104	272	274	284
5	Max. temp. in depth	^{o}C m (measured depth)	243 1320	104 1650	272 1780	274 1610	302 2025
6	Production: steam	t/h	18	-	26	23	57
7	Output	MWe	2	-	3	3	6

No	Data	Dimension	SBY-6	SBY-7	SBY-8	SBY-9	SBY-10
1	Type		Development	Development	Development	Development	Development
2	Elevation	m (above sea level).	1384	1384	1384	1337	1468
3	Total depth	m (vertical depth)	1750	2096	1935	1527	2164
4	Temp. at total depth	^{o}C	251	227	260	220	140
5	Max. temp. in depth	^{o}C m (measured depth)	270 1475	266 1600	270 1800	236 1350	170 400
6	Production: steam	t/h	33	23	36	15	-
7	Output	MWe	4	3	4	2	-